Applied Physics Express 12, 122001 (2019)
https://doi.org/10.7567/1882-0786/ab4b1b

LETTER

Single-step direct laser writing of halide perovskite microlasers

Ivan Shishkin[1*], Artem Polushkin[1], Ekaterina Tiguntseva[1], Aleksei Murzin[2], Boris Stroganov[2], Yury Kapitonov[2], Sergei A. Kulinich[3,4], Alexandr Kuchmizhak[3,5], and Sergey Makarov[1]

[1]ITMO University, St. Petersburg 197101, Russia
[2]Saint-Petersburg State University, ul. Ulyanovskaya 1, St. Petersburg 198504, Russia
[3]Far Eastern Federal University, Vladivostok 690091, Russia
[4]Department of Mechanical Engineering, Tokai University, Hiratsuka, Kanagawa 259-1292, Japan
[5]Institute of Automation and Control Processes (IACP), Far Eastern Branch of Russian Academy of Sciences, Vladivostok 690041, Russia

*E-mail: i.shishkin@metalab.ifmo.ru

Received July 31, 2019; revised September 25, 2019; accepted October 3, 2019; published online October 24, 2019

Halide perovskites are a family of materials with a high potential for realization of microlasers, due to their high luminescence quantum yield and broad spectral tunability. We demonstrate a single-step process for lasing microdisk fabrication from a thin film of methylammonium lead iodide ($MAPbI_3$) perovskite through its patterning with tightly focused femtosecond (fs) laser pulses. By using kHz-scale pulse bursts destructive overheating of the material was suppressed. Perovskite microdisks fabricated under such optimized conditions showed stable lasing upon pumping with fs-laser both at lower (50 kHz) and higher (80 MHz) repetition rates and operation temperatures of 300 K and 6 K, respectively.

Femtosecond (fs) laser ablation is a powerful, inexpensive and versatile method of patterning surfaces of various materials at the nano- and micro-scale.[1–12] However, microlasers made of conventional light-emitting semiconductor materials are hard to produce using fs-laser patterning because of possible material overheating and melting, as well as the formation of heat-induced defects that reduce quantum efficiency of luminescence. On the other hand, metal-halide perovskites present a novel class of promising materials with high defect tolerance, which makes their luminescence very efficient and, to some extent, robust to defects formation.[13] Therefore, such materials seem convenient for fabrication of light-emitting nano- and microstructures[14–16] and lasers.[17–20]

Although individual microscale perovskite lasers can be fabricated by low-cost chemical synthesis,[21] they cannot be arranged in a predefined way unless some additional multi-step lithography is applied to pattern either the substrate[22] or the perovskite.[23–25] At the same time, direct perovskite processing with a focused ion beam leads to harmful material amorphization and ion implantation, as well as defect formation in halide perovskites.[26] In this respect, direct fs-pulse patterning is seen as a promising technique for clean, inexpensive and straightforward processing of perovskites towards microlaser printing. In particular, inexpensive perovskite microdisk lasers with low lasing thresholds were recently produced using multi-pulse ablation of polycrystalline metal-halide perovskite films with a donut-shaped beam.[16] Despite the high quality and competitive characteristics of the perovskite microdisk lasers produced via such an approach, utilization of "structured" laser beams with a complex intensity profile substantially limits the fabrication flexibility and makes the approach less adoptable and suited for existing commercial ultra-fast setups and tools used for laser-processing.

In this letter, we report on direct fs-laser writing of perovskite microdisk lasers using conventional low-intensity Gaussian-shaped pulses. Two regimes of high-repetition rate (80 MHz) laser milling of perovskite microdisks, i.e. with and without additional temporal modulation (burst mode), were compared. It was found that the burst-mode laser milling allows to avoid overheating of microdisks' side-walls, thus resulting in their smoother morphology and supporting a stimulated emission amplification through the high-Q whispering gallery modes (WGMs). Remarkably, the microdisks fabricated by this method demonstrate lasing not only under standard optical pumping with pulsed radiation,[16] but also upon quasi-CW pumping, i.e. at 80 MHz fs-laser pumping, which is important for high-speed optical signal-processing.

In order to create thin films, we followed a protocol previously published elsewhere.[16] All the materials used in this study were as-received and without any additional purification. Lead(II) iodide (PbI_2, 99.99% trace metal basis, TCI Chemicals), methylammonium iodide (MAI, DYESOL), dymethyl sulfoxide (DMSO-1, ⩾99.5% (GC), Sigma-Aldrich; DMSO-2, anhydrous, ⩾99.8%, Alfa Aesar), N,N-dimethylformamide (DMF, anhydrous, ⩾99.8%, Sigma-Aldrich) and toluene (anhydrous, Sigma-Aldrich). PbI_2 (461 mg, 1 mmol) and MAI (159 mg, 1 mmol) were mixed and dissolved in DMSO-1 (170 mg, 0.154 ml) and DMF (610 mg, 0.646 ml) by shaking for 3 min to give a clear solution. The solution was filtered through a 0.45 μm PTFE syringe adapter and stirred on a hot plate for 30 min at 50 °C prior to perovskite film deposition. The rest of the solutions were treated in a similar way after their precursors were dissolved.

Glass substrates ($18 \times 18\,mm^2$) were subsequently sonicated in acetone and 2-propanol for 5 min, then washed with deionized water, and finally cleaned with O_3 for 5 min before film deposition. The $MAPbI_3$ perovskite films were spin-coated onto glass substrates by using an anti-solvent dripping method in a glove box. At the first cycle of spin-coating, the substrates were evenly covered with the corresponding perovskite ink, then spun at 300 rpm s^{-1} acceleration for 5 s and at 1500 rpm for the next 5 s. At the second stage, the rotation speed reached 2500 rpm during 1 s, where it was kept for 50 s. After 20 s of spinning, 100 μl of toluene was gently dripped onto the forming films, after which the films gradually changed their color during the next 30 s. The spin-coated films were annealed on a hot plate at 50 °C for 5 min and then at 80 °C for 10 min.

The microlaser fabrication process using the burst mode is schematically depicted in Fig. 1(a). We used a commercial laser system (M3D, Lazer Zentrum Hannover) to pattern the above mentioned perovskite films via laser beam scanning.

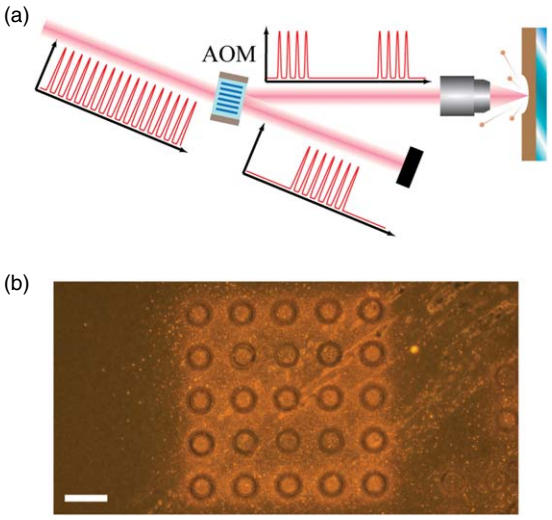

Fig. 1. (Color online) (a) Scheme of a few-pulse single-step direct laser writing of microdisks. The pulse train from femtosecond oscillator was thinned with acousto-optical modulator with adjustable open time. (b) Photoluminescence image of a $MAPbI_3$ perovskite film with milled microdisks. Scale bar indicates 20 μm. Scale bar indicates 10 μm.

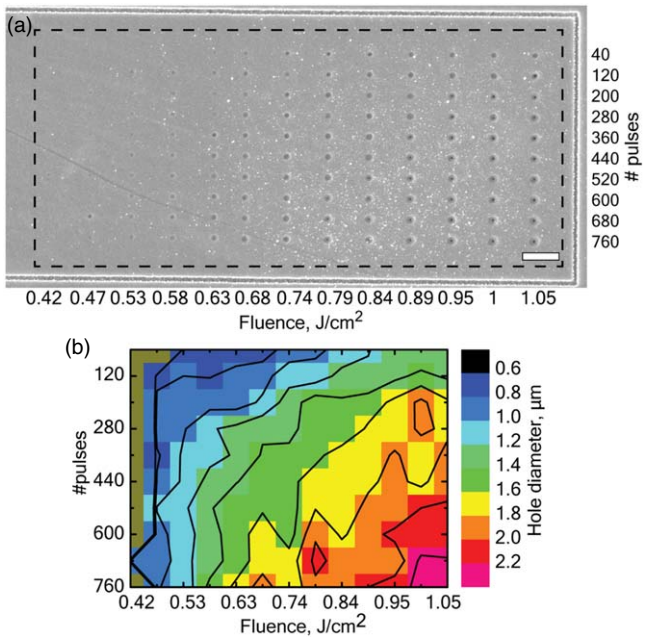

Fig. 2. (Color online) (a) SEM image of $MAPbI_3$ film with holes fabricated at various laser fluences and number of pulses. (b) Experimental dependence of hole diameter on laser fluence and number of pulses presented as a 2D color map. Scale bar indicates 10 μm.

Laser pulses (with central wavelength 800 nm and pulse duration 100 fs) from a Ti:Sa oscillator (TiF-100F) focused by $40 \times \mathrm{NA} = 0.7$ objective into a spot with diameter of 0.7 μm were used for such multi-pulse ablation. A few-pulse bursts were obtained by using an acousto-optical modulator (AOM, Gooch and Housego) operating as a high-speed shutter, where only radiation diffracted to the 1st order by the AOM was delivered to the sample film [Fig. 1(a)]. The minimum open time was 1 μs, which corresponds to ≈60–80 pulses hitting the sample. The sample was scanned along circular trajectories of variable diameter ranging from 2 to 10 μm at 1 μm step, with a scanning velocity being of 50 μm s^{-1} for 20 cycles. The duty cycle (shutter on/off time) was chosen so that the exposed spots would overlap by half beam diameter for a given beam spot size and scanning velocity.

The applied regime of direct laser writing allowed the fabrication of milling arrays of isolated perovskite microdisks, shown in Fig. 1(b), which are promising for real applications. However, longer laser exposition periods led to a large amount of ablative remnants in the form of nanoparticles, which caused brighter photoluminescence signals from the covered area via the Purcell factor enhancement at Mie resonances of the isolated nanoparticles [see Fig. 1(b)], as was described in our previous works.[14,15)]

In order to optimize the microdisk milling process, we carried out a systematic study on thin film ablation by laser under different experimental conditions. Figure 2(a) shows an SEM image of film area with through microholes of different diameters milled using the burst mode at variable laser fluence and with a different number of pulses. Figure 2(b) presents the microhole diameter as a function of these two parameters in a form of color-coded map. Analysis of the experimental data reveals that the hole diameter expectedly depends on both the number of applied pulses and laser fluence, being varied from 0.6 to 2.2 μm for a fixed size of optical spot. The results in Fig. 2 were obtained with temporal modulation of the laser beam as shown in Fig. 1(a), which turned out to be much more preferable for lasing applications. The most optimal regime for reproducible and relatively clean laser ablation is shown by green and yellow bands in Fig. 2(b), corresponding to fluence values around 0.55–0.7 J cm^{-2} and around 0.7–1.05 J cm^{-2} at higher and lower number of pulses, respectively. This is typical behavior for ablation of semiconductors with a femtosecond laser.[1,27)] In sharp contrast, laser patterning without AOM modulation of the pulse train is known to result in larger hole sizes and, most likely, in thermal degradation of the material.

Figure 3 compares two perovskite microdisks produced at quasi-CW exposure at an average fluence of 0.08 J cm^{-2} [Fig. 3(a)] and under burst-mode ablation at an average fluence of 0.8 J cm^{-2} [Fig. 3(b)] and constant scanning speed of 50 μm s^{-1}. Even though the quasi-CW milling mode is seen to yield less ablative remnants, it produced rougher sidewalls of the microdisk and, presumably, strongly overheated the surrounding perovskite material. These two factors are believed to prevent the appearance of any features related to lasing from such microdisks. In turn, burst-mode printing did not deteriorate the light-emitting properties of perovskite material within the microdisk, resulting in lasing observed under appropriate pumping, as will be discussed in more detail below.

First, the lasing performance of fabricated microdisks was tested under femtosecond laser photoexcitation with a relatively low repetition rate (interpulse time much longer than carriers relaxation in $MAPbI_3$[28)]) and at room temperature.[29)] A second harmonic (wavelength 525 nm and pulse duration 150 fs) generated from a femtosecond laser oscillator (TeMa, Avesta Project) was used as an excitation source. In order to minimize the influence of thermal effects on lasing characteristics of the microdisks, pulse repetition rate was reduced down to 25 kHz using a pulse picker. The pumping

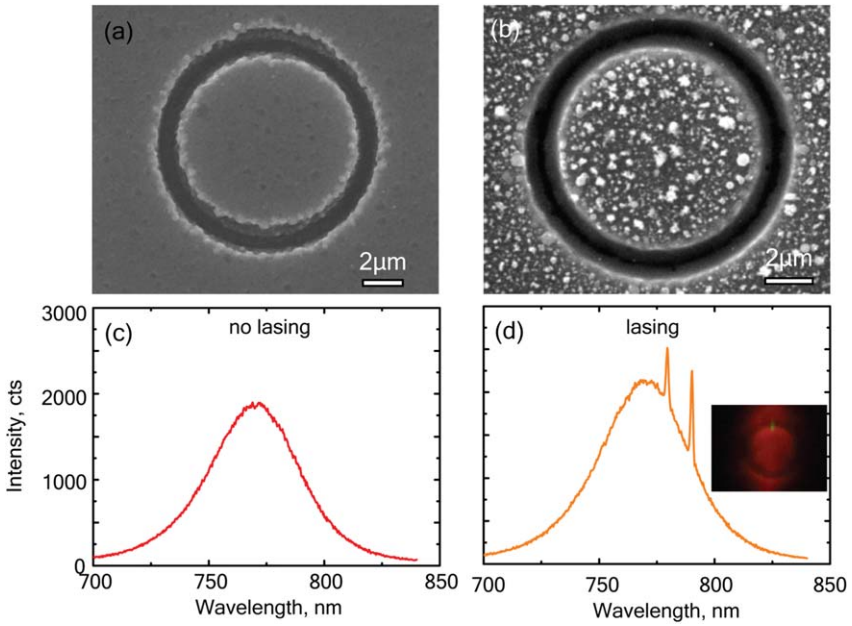

Fig. 3. (Color online) (a), (b) Comparative SEM images and (c), (d) photoluminescence spectra of two microdisks fabricated at quasi-CW (left) and burst regimes (right). Optical image of lasing from the microdisk is shown as inset in Fig. 3(d).

laser radiation was focused on the sample using a $10 \times \mathrm{NA} = 0.28$ objective (Mitutoyo) with a glazing angle of incidence equal to 65°. The light was collected using a $50 \times \mathrm{NA} = 0.42$ objective (Mitutoyo) and analyzed using a confocal spectrometer (Horiba LabRam) equipped with gratings (150 and 1800 grooves mm^{-1}). Typical spectra obtained at excitation fluence of 0.5 mJ cm^{-2} are shown in Figs. 3(c), 3(d) with the corresponding optical image given as an inset in Fig. 3(d).

Comparison of the quasi-CW and burst milling of perovskite films suggests that the two regimes of the laser ablation are quite different with respect to fabricated microsctructures on the surface of perovskite film. Moreover, their products also differ from those obtained via ablation of conventional metals or semiconductors.[30–34] First of all, the thermal conductivity of $MAPbI_3$ (0.5–0.68 W m^{-1}·K at room temperature[35,36] is several orders of magnitude lower than those for silicon and gold. Second, $MAPbI_3$ is an organic-inorganic material that can be dissociated due to photochemical reaction at temperatures (incident laser fluences) well below its melting point. In particular, a possible pathway for such a decomposition under illumination in the presence of moisture includes its decomposition to PbI_2 and MAI, with further dissociation of the latter to methylamine, iodine and water molecules,[37] or to PbI_2, MA, HI and H_2O.[38] Some photochemical mechanisms are likely to be dominant for laser milling at high repetition rate, resulting in clean material removal [Fig. 3(a)]. At the same time, the explosive-like regime of laser ablation without gradual heat accumulation is more likely to be the case for Fig. 3(b) as the ablative debris observed around the microdisk resemble droplets.

For microlaser operations, one of the most challenging regimes is known to be its photoexcitation with a high repetition rate which is shorter than the typical time for free carriers relaxation in perovskites (≈10–100 ns[28]). Usually, such an excitation can result in a thermal degradation of the perovskite microdisk before reaching its stable lasing regime. Therefore, low-temperature conditions are required. Moreover, at temperatures below 150 K there is a phase transition from tetragonal to orthorhombic $MAPbI_3$, which is beneficial for lasing because the coexistence of these two phases and inclusion of the tetragonal phase were found to facilitate higher gain.[39]

In our experiments, photoluminescence spectra were collected from a perovskite microdisk cooled down to $T = 6$ K using a closed-loop helium cryostat (Montana cryostation). A tunable Ti:Sa laser (Spectra Physics MaiTai HP) was used to excite the samples. The pumping emission wavelength was tuned to 746.7 nm, providing a pulse train with a pulse width of 150 fs and frequency of 80 MHz. The incident laser intensity was varied using gradient ND filter. The laser was focused using a long-working-distance objective with a magnification of ×20. The laser light was coupled to the objective by a 50:50 beam-splitter cube. The excitation laser was suppressed by two polarizers inserted in the detection path. The collected emission was analyzed by a spectrometer (MDR-4) with gratings of 1200 grooves mm^{-1}.

Figure 4(a) confirms a threshold-like behavior for two lasing modes in a perovskite microdisk with a diameter of 7 μm observed at $T = 6$ K. The modes can be attributed to the type of WGMs, considerably affected by roughness, according to the previous calculations for perovskite microdisks.[16] Some blue-shift of the modes and PL spectral position from 765 nm to 760 nm [Fig. 4(b)] can be attributed to the overheating of the perovskite material by laser beam with an average power around 1.5 mW.[40] Figures 4(c)–4(d) allow the determination the lasing threshold values for each mode, which are almost equal (being ≈21 μJ cm^{-2}), by finding the fluence of sharp PL narrowing from 10 nm to 0.4 nm, as well as the fluence, where the signal intensity demonstrates a kink. The kink is not very clear because of the specific of our experimental arrangement registering mostly scattered light from the microdisks rough walls and central parts to the vertical direction, whereas lasing emission at

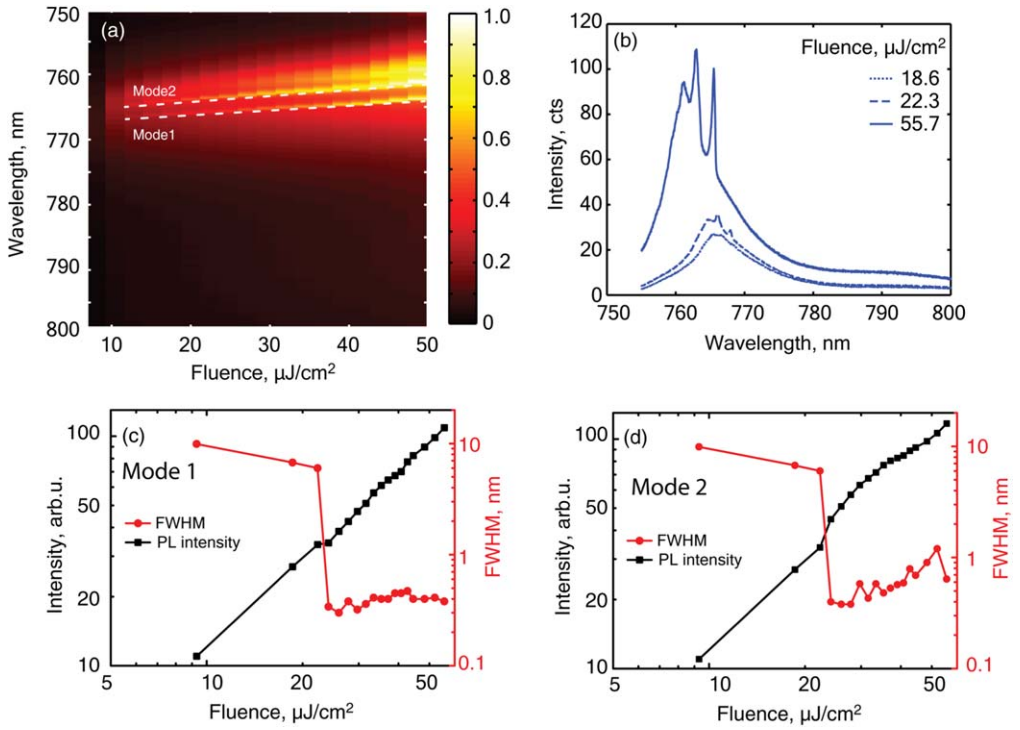

Fig. 4. (Color online) (a) Photoluminescence map of microdisks pumped with femtosecond oscillator at 6 K (quasi-CW excitation). (b) Photoluminescence spectra obtained at variable pumping fluence. Intensity and peak full width at half-maximum plotted versus fluence for lower-energy lasing mode (Mode 1) (c), and for higher-energy lasing mode (Mode 2) (d).

WGMs should be predominantly out-coupled in a plane parallel to the film surface.[16,41] In such cases, strong contribution of spontaneous emission not coupled into the lasing modes gives a pedestal to the emission spectrum making the kink in the light–light curves weaker as compared with the experimental conditions, where the lasing mode is selectively pumped and collected, while the spectral narrowing is pronounced in both cases.[42]

Generally, the regime of optical pumping with MHz-rate excitation in our work can be compared with previous studies on quasi-CW and CW photoexcitation, where lasing thresholds were in the range of average intensities 5–20 kW cm^{-2} for $MAPbI_3$,[39,43] and 0.4 kW cm^{-2} for a phase-stable mixed-cationic perovskite.[44] According to Figs. 4(c), 4(d), lasing thresholds in our experiments at low temperature are around 3 kW cm^{-2}, being close to the data from the literature. Additional stability tests show that lasing operation does not get worse, at least during 10^7 pulses at room temperature and 10^{11} pulses at T = 6 K, which is consistent with previous studies.[16,44–47]

To summarize, we developed a novel approach for the fabrication of perovskite-microdisk lasers by employing direct fs-pulse burst-mode laser patterning of $MAPbI_3$ thin films. The optimized laser printing conditions allowed to produce high-quality perovskite microdisks with smooth sidewalls at minimized thermal damage of the material within the disk. As a result, we observed both stable room-temperature lasing from the microdisks under their kHz-rate pumping and lasing from similar microdisks cooled down to cryogenic temperatures under MHz-rate excitation. The proposed method of microdisk printing is quite universal with respect to perovskite composition. Therefore, our findings pave the way to a fast, scalable and cost-effective fabrication of perovskite microlasers in a fully controllable manner, which is important for advanced photonic applications.

Acknowledgments This work was supported by the Ministry of Education and Science of the Russian Federation (project 14.Y26.31.0010), for thin films preparation and optical measurements, and the Russian Science Foundation (project 19-19-00177), for experiments on laser ablation. We also acknowledge the SPbU Resource Centers "Nanophotonics" where the part of experiments was carried out.

ORCID iDs Ivan Shishkin https://orcid.org/0000-0002-2330-0159 Sergei A. Kulinich https://orcid.org/0000-0002-1365-9221 Sergey Makarov https://orcid.org/0000-0002-9257-6183

1) D. W. Bäuerle, *Laser Processing and Chemistry* (Springer, Berlin, 2013).
2) J. Bonse, J. Krüger, S. Höhm, and A. Rosenfeld, J. Laser Appl. **24**, 042006 (2012).
3) A. A. Ionin, S. I. Kudryashov, S. V. Makarov, L. V. Seleznev, D. V. Sinitsyn, E. V. Golosov, A. G. Ol'ga, Y. R. Kolobov, and A. E. Ligachev, Applied Physics A **107**, 301 (2012).
4) A. Y. Vorobyev and C. Guo, Laser & Photonics Reviews **7**, 385 (2013).
5) C. S. Nathala, A. Ajami, A. A. Ionin, S. I. Kudryashov, S. V. Makarov, T. Ganz, A. Assion, and W. Husinsky, Optics Express **23**, 5915 (2015).
6) C. Kerse et al., Nature **537**, 84 (2016).
7) A. Kuchmizhak, E. Pustovalov, S. Syubaev, O. Vitrik, Y. Kulchin, A. Porfirev, S. Khonina, S. Kudryashov, P. Danilov, and A. Ionin, ACS Applied Materials & Interfaces **8**, 24946 (2016).
8) S. Makarov et al., Nanoscale **8**, 17809 (2016).
9) S. Syubaev, A. Zhizhchenko, A. Kuchmizhak, A. Porfirev, E. Pustovalov, O. Vitrik, Y. Kulchin, S. Khonina, and S. Kudryashov, Optics Express **25**, 10214 (2017).
10) O. Tokel et al., Nature Photonics **11**, 639 (2017).
11) E. Gamaly, S. Juodkazis, and A. Rode, Nanomaterials **8**, 555 (2018).
12) X.-W. Cao, Q.-D. Chen, H. Fan, L. Zhang, S. Juodkazis, and H.-B. Sun, Nanomaterials **8**, 287 (2018).
13) R. E. Brandt, J. R. Poindexter, P. Gorai, R. C. Kurchin, R. L. Hoye, L. Nienhaus, M. W. Wilson, J. A. Polizzotti, R. Sereika, and R. Zaltauskas, Chem. Mater. **29**, 4667 (2017).
14) E. Tiguntseva, G. Zograf, F. Komissarenko, D. Zuev, A. Zakhidov, S. Makarov, and Y. S. Kivshar, Nano Letters **18**, 1185 (2018).

15) E. Y. Tiguntseva, D. G. Baranov, A. P. Pushkarev, B. Munkhbat, F. Komissarenko, M. Franckevicius, A. A. Zakhidov, T. Shegai, Y. S. Kivshar, and S. V. Makarov, Nano Letters **18**, 5522 (2018).
16) A. Zhizhchenko et al., ACS Nano **13**, 4140 (2019).
17) B. R. Sutherland and E. H. Sargent, Nature Photonics **10**, 295 (2016).
18) S. Makarov, A. Furasova, E. Tiguntseva, A. Hemmetter, A. Berestennikov, A. Pushkarev, A. Zakhidov, and Y. Kivshar, Adv. Opt. Mater. **7**, 1800784 (2018).
19) Y. Gao et al., ACS Nano **12**, 8847 (2018).
20) Q. Wei, X. Li, C. Liang, Z. Zhang, J. Guo, G. Hong, G. Xing, and W. Huang, Adv. Opt. Mat. **7**, 1900080 (2019).
21) E. Y. Tiguntseva, K. L. Koshelev, A. D. Furasova, V. Y. Mikhailovskii, E. V. Ushakova, D. G. Baranov, T. O. Shegai, A. A. Zakhidov, Y. S. Kivshar, and S. V. Makarov, (2019), (arXiv:1905.08646).
22) P. Liu, X. He, J. Ren, Q. Liao, J. Yao, and H. Fu, ACS Nano **11**, 5766 (2017).
23) N. Zhang, W. Sun, S. P. Rodrigues, K. Wang, Z. Gu, S. Wang, W. Cai, S. Xiao, and Q. Song, Adv. Mater. **29**, 1606205 (2017).
24) X. Yang, J. Wu, T. Liu, and R. Zhu, Small Methods **2**, 1800110 (2018).
25) P. J. Cegielski et al., Nano Letters **18**, 6915 (2018).
26) Y. Wang, Z. Gu, Y. Ren, Z. Wang, B. Yao, Z. Dong, G. Adamo, H. Zeng, and H. Sun, ACS Appl. Mater. Interfaces **11**, 15756 (2019).
27) J. Bonse, S. Baudach, J. Krüger, W. Kautek, and M. Lenzner, Applied Physics A **74**, 19 (2002).
28) S. D. Stranks, V. M. Burlakov, T. Leijtens, J. M. Ball, A. Goriely, and H. J. Snaith, Physical Review Applied **2**, 034007 (2014).
29) F. Deschler et al., J. Phys. Chem. Lett. **5**, 1421 (2014).
30) B. N. Chichkov, C. Momma, S. Nolte, F. Von Alvensleben, and A. Tünnermann, Applied Physics A **63**, 109 (1996).
31) N. Bulgakova and A. Bulgakov, Applied Physics A **73**, 199 (2001).
32) R. Stoian, A. Rosenfeld, D. Ashkenasi, I. Hertel, N. Bulgakova, and E. Campbell, Physical Review Letters **88**, 097603 (2002).
33) M. Malinauskas, A. Žukauskas, S. Hasegawa, Y. Hayasaki, V. Mizeikis, R. Buividas, and S. Juodkazis, Light: Science & Applications **5**, e16133 (2016).
34) A. A. Ionin, S. I. Kudryashov, and A. A. Samokhin, Physics-Uspekhi **60**, 149 (2017).
35) A. Pisoni, J. Jacimovic, O. S. Barisic, M. Spina, R. Gaál, L. Forró, and E. Horváth, The Journal of Physical Chemistry Letters **5**, 2488 (2014).
36) S. Sugawara, T. Sato, T. Takahashi, T. Isobe, A. Nakajima, and S. Matsushita, Materials Research Innovations **23**, 49 (2019).
37) G. Niu, W. Li, F. Meng, L. Wang, H. Dong, and Y. Qiu, Journal of Materials Chemistry A **2**, 705 (2014).
38) J. M. Frost, K. T. Butler, F. Brivio, C. H. Hendon, M. Van Schilfgaarde, and A. Walsh, Nano Letters **14**, 2584 (2014).
39) Y. Jia, R. A. Kerner, A. J. Grede, B. P. Rand, and N. C. Giebink, Nature Photonics **11**, 784 (2017).
40) E. Tiguntseva et al., Applied Surface Science **473**, 419 (2019).
41) S. McCall, A. Levi, R. Slusher, S. Pearton, and R. Logan, Applied Physics letters **60**, 289 (1992).
42) G. Björk, H. Heitmann, and Y. Yamamoto, Physical Review A **47**, 4451 (1993).
43) Y. Jia, R. A. Kerner, A. J. Grede, A. N. Brigeman, B. P. Rand, and N. C. Giebink, Nano Letters **16**, 4624 (2016).
44) P. Brenner, O. Bar-On, M. Jakoby, I. Allegro, B. S. Richards, U. W. Paetzold, I. A. Howard, J. Scheuer, and U. Lemmer, Nature Communications **10**, 988 (2019).
45) G. Xing, N. Mathews, S. S. Lim, N. Yantara, X. Liu, D. Sabba, M. Grätzel, S. Mhaisalkar, and T. C. Sum, Nature Materials **13**, 476 (2014).
46) P. Brenner, M. Stulz, D. Kapp, T. Abzieher, U. W. Paetzold, A. Quintilla, I. A. Howard, H. Kalt, and U. Lemmer, Applied Physics Letters **109**, 141106 (2016).
47) P. Brenner, T. Glöckler, D. Rueda-Delgado, T. Abzieher, M. Jakoby, B. S. Richards, U. W. Paetzold, I. A. Howard, and U. Lemmer, Optical Materials Express **7**, 4082 (2017).